Jurnal Penelitian Fisika dan Aplikasinya (JPFA)
Volume 13, Issue 02, December 2023
https://journal.unesa.ac.id/index.php/jpfa/

p-ISSN: 2087-9946
e-ISSN: 2477-1775

Altering Coconut Shell Biomass to High-Ordered Graphitic Carbon with Nickel Catalyzation

Biaunik Niski Kumila [1,a,*], Farhan Adityaa [1,b], Fredina Destyorini [2,c], Fitri Nur Indah Sari [3,d], Dhita Azzahra Pancorowati [4,e], and Hamdan Hadi Kusuma [5,f]

[1] Department of Physics, Faculty of Science and Technology, UIN Syarif Hidayatullah
Jalan Ir H. Juanda No. 95, Ciputat, South Tangerang 15412, Indonesia
[2] Research Center of Nanotechnology and Materials, National Research and Innovation Agency
Jalan Raya Puspiptek Setu Serpong, South Tangerang 15314, Indonesia
[3] Department of Materials Science and Engineering, Faculty of Engineering,
National Cheng Kung University
No. 1 Dasyue Rd, East District, Tainan City 701, Taiwan
[4] Department of Energy Science and Engineering,
Daegu Gyeongbuk Institute of Science and Technology
Daegu Gyeongbuk, Dalseong-gun, Daegu, South Korea
[5] Department of Physics, Faculty of Science and Technology, Walisongo State Islamic University
Jalan Walisongo No.3-5, Tambakaji, Ngaliyan, Semarang 50185, Indonesia

e-mail: [a] biaunik@uinjkt.ac.id, [b] farhan.luhfi18@mhs.uinjkt.ac.id, [c] fredina.destyorini@lipi.go.id, [d] fitrinurindah_26@yahoo.com, [e] dhita_169@dgist.ac.kr, and [f] hamdanhk@walisongo.ac.id
* Corresponding Author

Received: 23 August 2023; Revised: 30 October 2023; Accepted: 3 November 2023

Abstract

Graphite is a carbon-based material potentially utilized in numerous applications, such as electrodes for supercapacitors, lithium-ion batteries, and absorbers for water treatment. Biomass graphite is a beneficial candidate for low-cost yet valuable graphite. In this work, coconut shells, the abundant materials with high carbon contents, were successfully transformed into valuable coconut shell graphite (CSG) using metal catalytic graphitization with nickel as a catalyst at low-temperature conditions of ~1200 °C. Nickel concentration varied between 2 mmol, 3 mmol, and 5 mmol per gram of carbon. The samples were further examined using X-ray diffraction (XRD), Raman Spectroscopy, and Transmission Electron Microscope (TEM). The high graphitization degree of ~ 72 % was confirmed by X-ray diffraction analysis. That was further supported by the high-ordered stacking carbon layer that appeared in HR-TEM images. Meanwhile, Raman spectroscopy confirms that nickel impregnation diminished the structural defect of samples and increased the sp^2-carbon bond indicated by its rise of IG/ID. The IG/ID values of CGS and CGS-Ni_{5mmol} are 0.86 and 0.92, respectively.

Keywords: *Biomass Graphite; Coconut Shells; Nickel Catalyzation*

DOI: 10.26740/jpfa.v13n2.p119-131

How to cite: Kumila BN, et al. Altering Coconut Shell Biomass to High-Ordered Graphitic Carbon with Nickel Catalyzation. *Jurnal Penelitian Fisika dan Aplikasinya (JPFA)*. 2023; **13**(2): 119-131.

INTRODUCTION

Graphite is a desirable byproduct of biochar and is utilized in various processes. Due to its excellent electrical conductivity, graphite can be employed as electrochemical electrodes [1–3] and as an anode for secondary batteries [4–7]. Due to its high melting point characteristics, graphite is also a good material for the casting and molding sector [8]. Its market expansion is anticipated to be fueled by the rising demand for Li-ion grade graphite [9–11] to meet the needs of electric vehicles (EVs). However, despite all of graphite's outstanding properties and widespread applications, it is a mineral resource that is irregularly distributed on Earth and is synthesized artificially at high operation temperature (~3,000 °C) from coal called the Acheson technique [12]. Therefore, high-cost production and limited natural supply are the main causes of concern. In order to address those problems, many researchers have been developing biomass-derived carbon as a potential precursor for graphite due to its abundant supply, benign effects on the environment, and inexpensive cost [13–15].

Due to the ease of manufacture, affordability, and sustainability, biomass-derived graphite has attracted much interest among researchers. Numerous biomass products have been utilized as precursors, such as chitin and cellulose rich-precursors [16], grape extract [17], coconut waste [18], and oil palm empty fruit bunch (EFB) [19,20] in various ways [21] to prepare graphite. Among all carbonaceous precursors, carbon phases generated from coconut shell charcoal have several beneficial properties, including their mesoporous structure [22], hardness [23], and electronic conductivity [24].

Coconut shell (CS) is an agricultural waste broadly available in India, Indonesia, the Philippines, and Sri Lanka, which are primarily the top coconut producers. The underused coconut shell trash is burned outside or dumped in ponds, which pollutes the environment [25]. Because of its chemical characteristics, CS fiber can improve novel composites and give them higher strength and modulus properties [26]. The components of a coconut shell are cellulose (26.6%), hemicellulose (21%), lignin (29.4%), pentosans (27.7%), solvent extractives (4.2%), uronic anhydrides (3.5%), and ash (0.6%) [27]. Due to its high porosity and surface area, coconut shell-activated carbon is frequently employed as an adsorbent [28]. Coconut shells are also effectively utilized to produce charcoal and activated carbon due to their high carbon content (49.86%) [25].

The Acheson technique is still used to convert amorphous carbon to graphite, which requires an energy-intensive process that leads to the graphite's high cost [12]. Therefore, developing a technique that converts traditionally non-graphitizable carbon precursors into highly ordered graphitic structures at lower temperatures is still challenging. Numerous techniques are currently used to produce graphitic carbon structure generated from biomass, such as pyrolysis, chemical activation, mainly KOH [29], and catalytic graphitization utilizing transition metals such as Fe, Co, and Ni as catalysts [30–34]. The primary techniques for creating carbon compounds from biomass with a great graphitic structure are high-temperature pyrolysis and catalytic graphitization [35] since the graphitic structure of biomass with chemical activation has low electrical conductivity [16].

Numerous methods have been developed for graphite using coconut shells as a precursor [24,36–38]. However, the successful conversion of highly disordered amorphous carbon from coconut shells to high-ordered graphite reported by previous studies is still challenging and has not been well discovered. Therefore, in this report, we propose efficient metal catalysis using nickel as a catalyst that successfully transformed the amorphous carbon from coconut shells into high-ordered graphite at low temperatures.

METHOD

The three main synthesis steps are preparing coconut shell powder, impregnating nickel, and pyrolysis/heat treatment to produce the graphitic carbon phase. In this section, these three processes are described in extensive detail. This section also describes the materials and research methods, including the tools and equipment employed.

Material Synthesis

Preparation of Coconut Shell Carbon

After being cleansed to remove impurities, the carbon derived from the coconut shell powder was dried in a vacuum oven at 60 °C. A 200-mesh sieve was then utilized to refine and filter the powder. The coconut shell powder was then heated at 500 °C for an hour under a nitrogen atmosphere to complete the carbonization process.

Nickel Impregnation Process

The graphitic carbon derived from coconut shells was synthesized by metal catalytic graphitization using nickel as a catalyst. The 5 g of coconut shell carbon was dissolved in deionized water. Nickel (II) chloride hexahydrate ($NiCl_2.6H_2O$) was added to the carbon solution, with a concentration of 2 mmol, 3 mmol, and 5 mmol of nickel per gram of carbon. The mixture was then stirred at 60 °C and dried overnight. The solution was then heated at 110 °C to remove the remaining solvent.

Synthesis of Coconut Shell-Graphite (CSG)

The as-synthesized carbon impregnated by nickel was then graphitized at 1200 °C under nitrogen flow for 3 hours. The sample was then washed with HCl 40% to remove nickel impurities. The product mixture was further washed with DI water until it reached normal pH and dried to produce graphitic carbon powder. The product was then labeled as CSG-Ni. In contrast, the sample without nickel impregnation was labeled as CSG.

Material Characterization

The samples (CSG and CSG-Ni) were further examined with X-ray diffraction (XRD), Raman spectroscopy, and transmission electron microscopy (TEM) as described in this section. X-ray diffraction (XRD) was used to analyze the structural phase, defining the degree of graphitization and height of stacked layer carbon. The degree of graphitization was calculated by Equation 1 [39,40].

$$DOG = (3.440 - d_{(002)})/(3.440 - 3.354) \quad (1)$$

where DOG is the degree of graphitization, 3.440 is the interplanar spacing of turbostratic graphite, $d_{(002)}$ is the interplanar spacing of the sample, and 3.354 is the interplanar spacing of single crystal graphite. The crystallite size (L_c) was calculated using Equation 2, Scherrer equation [39,41].

$$Lc = (K\lambda)/(\beta cos\theta) \quad (2)$$

where λ is the source radiation wavelength of Cu Kα, β is the full width at half maxima (FWHM) of XRD peak at 2θ, and K is the dimensionless constant which depends on the reflection plane. In this case, K for the (002) plane is 0.89. The number of stacked carbon layers was also calculated by Equation 3.

$$n = \frac{Lc}{d_{002}} \quad (3)$$

In order to observe the degree of structural defect of samples, Raman spectroscopy analysis was carried out with a Raman iHR320 Horiba spectrometer equipped with an Argon laser source (514 nm). Moreover, the Transmission Electron Microscope (TEM) studies were carried out to provide an actual image of stacking layered graphite. Furthermore, the Selected Area Diffraction (SAED) technique was also employed to observe the lattice parameter.

RESULTS AND DISCUSSION

Figure 1 shows the XRD patterns of CSG and CSG-Ni. Figure 1(a) shows the raw XRD data from all samples, whereas Figure 1(b) shows the smoothed data fit and subjected to peak analysis. As can be observed from Figure 1, CSG shows two broad peaks at approximately 2θ = 23.54^0 and 43.89^0, respectively, indicating its amorphous carbon structure. Furthermore, the XRD pattern of CSG-Ni_{2mmol} shows a similar feature as CSG. Therefore, CSG and CSG-Ni_{2mmol} exhibit an amorphous carbon structure. In contrast, CSG-Ni_{3mmol} and CSG-Ni_{5mmol} reveal an additional sharp peak at approximately 2θ = 26°, contributing to the graphitic crystalline plane of (002). Moreover, the peak at approximately 2θ = 43°-44° indicates the (101) plane. Figure 1 (c) shows the convolution result of the important peak at 2θ = 23.54°, corresponding to (002). Graphitic carbon's diffraction properties typically result in a strong peak around 2θ = 24° [30,39,42,43]. The sample diffraction data from this study for CGS-Ni_{3mmol} and CGS-Ni_{5mmol} (Figure 3(c), however, revealed two peaks made up of a broad peak (blue) and a sharp peak (green). The broad peak (blue) corresponds to the disordered graphite phase, while the sharp peak (green) demonstrates the high-ordered graphitic phase. Moreover, the red peak shows the cumulative fit-peak of all peaks. Previous studies have found similar findings for the diffraction features of biomass graphite, which is related to the turbostratic graphitic phase [1,18,21,34]. Turbostratic carbon is typically considered a variation of h-graphite, and both the h-graphite and the t-carbon are piled up by graphene layers with uniform spacing but varied stacking ordering degrees. Although the graphene layers of t-carbon may arbitrarily translate to each other and rotate around the normal of the graphene layers, h-graphite has an ordered AB stacking structure [39,44].

In conclusion, a sufficient concentration of nickel improves the degree of graphitization, proved by the appearance of a sharp peak of the (002) plane, confirming that the sp^2 carbon bond is optimized after nickel catalyzation (see Figure 2). Furthermore, the XRD data shows the successful transformation of biomass to highly ordered graphitic carbon after the nickel catalyzation process at a relatively low temperature (~1200 °C) compared to the ancient high-cost graphitization process, which was performed at high temperatures up to 3000 °C. Metals such as copper, iron, cobalt, and nickel have been commonly utilized as catalysts to reduce the graphitization temperature of biomass carbon [30]. However, enhancing the quality of crystalline graphite as measured by the degree of graphitization (DOG) remains a problem in the commercialization of biomass graphite.

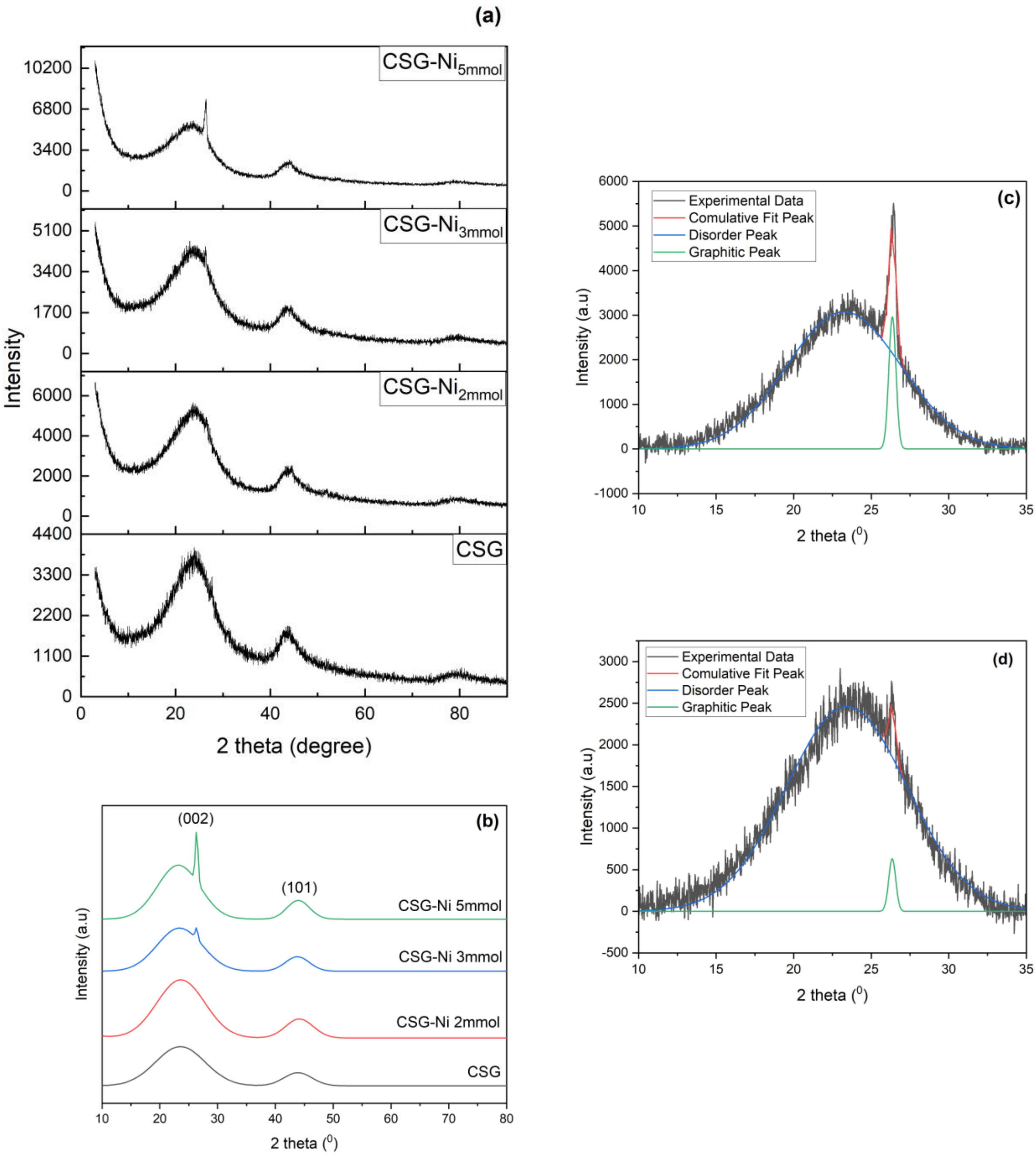

Figure 1. Raw Experimental XRD Result of (a) CSG and CSG-Ni in Various Concentrations; (b) Cumulative-fit Peak of CSG and CSG-Ni with Various Concentrations, (c) Convolution Peak of CSG-Ni_{5mmol}; and (d) CSG-Ni_{3mmol}

Research conducted by Fredina et al. stated that a DOG of 77.9% was successfully achieved in the coconut fiber graphitization process using nickel as a catalyst at a graphitization temperature of 1300 °C [34]. In this study, a new precursor, coconut shell, was successfully graphitized at a lower temperature of 1200 °C, resulting in a DOG of 71.96% (see Table 1). Previous researchers have carried out coconut shell graphitization using various methods [24,36,38,45,46]. However, those earlier publications lacked solid evidence to support the finding that high crystalline-graphite formation was successful. In other words, the graphitization of coconut shells used in earlier studies results in low-crystalline or amorphous-grade graphite graphite. Therefore, employing the nickel catalyzation process at low temperatures, this research can be a starting point for successfully synthesizing high-ordered graphite from coconut shells.

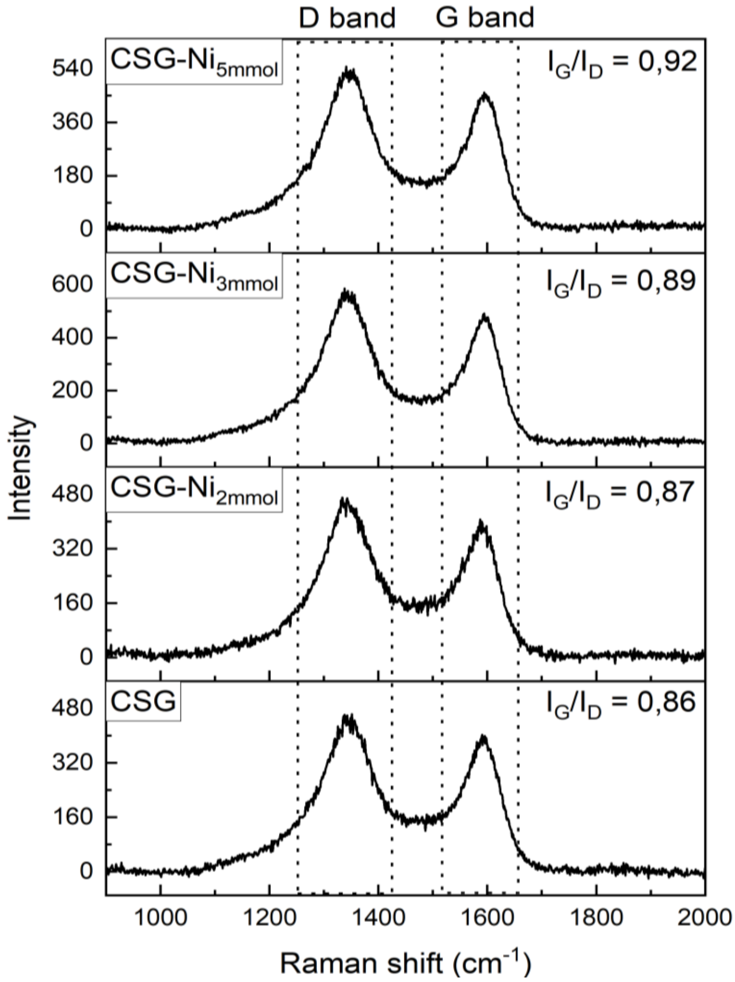

Figure 2. Raman Spectra of CSG and CSG-Ni in Various Concentrations

Table 1. Structural Parameters of Samples Obtained from XRD Data Analysis

Parameters	Samples			
	CSG	CSG-Ni_{2mmol}	CSG-Ni_{3mmol}	CSG-Ni_{5mmol}
Phase	Amorphous	Amorphous	Graphitic	Graphitic
Degree of Graphitization (DOG), (%)	-	-	70.42	71.96
Interlayer spacing of (002), (d_{002}), (nm)	-	-	0.338	0.337
Crystallite size (L_c), (nm)	-	-	15.10	14.89
Number of stacked layers (n)	-	-	44.68	44.10

The parameters calculated from XRD data analysis, including degree of graphitization, crystallite size/number of stacked layer graphite, and lattice parameter of samples, are concluded in Table 1. The high-ordered biomass graphite with a degree of graphitization up to~72% was obtained by CSG-Ni_{5mmol}, which is the great DOG compared to previous works [24,36].

The Raman spectrum is used to identify further the structure, specifically the existence of defects in samples. Figure 2 shows two distinct peaks: the D band (~ 1350 cm^{-1}) and the G band (~1590 cm^{-1}), corresponding to the disordered carbons and sp^2 bonded carbon atoms, respectively. Defects generally consist of physical or structural defects and chemical defects. Physical defects are associated with structural damage due to the presence of pores, holes, and vacancies in the sample. At the same time, carbon bonds cause chemical defects with oxygen functional groups such as epoxy, hydroxyl, carboxylic, and carboxyl groups [47,48].

Graphite is a carbon-sp^2 bond that is arranged hexagonally. Any form of arrangement of carbon bonds other than sp^2, such as sp^3 and sp, is also categorized as a chemical defect [49,50]. The G peak in Raman is associated with the sp^2 quantity of carbon in the sample, while the D peak is associated with all types of physical and chemical defects. I_G and I_D are related to the intensity of the G and D peaks, respectively. Therefore, I_G/I_D is a value of the G and D peak intensity ratio, representing the amount of sp^2-carbon bond and the quality of the sample. The greater the I_G/I_D value, the higher the quality of the graphitic carbon. The intensity ratio of the G and D band (I_G/I_D) indicates the degree of sp^2 bonded carbon of materials. The I_G/I_D values of CSG in CSG-Ni_{2mmol}, CSG-Ni_{3mmol}, and CSG-Ni_{5mmol} are 0.86, 0.87, and 0.89, respectively. After nickel impregnation, the increasing I_G/I_D value of samples indicates a higher number of sp^2-bonded carbon, confirming the rise in graphitization degree. This statement further supports the XRD analysis, which expresses that nickel catalyzes graphitization to occur.

TEM images are used to analyze the atomic morphology of the material further. Figure 3(a-c) shows the TEM images of CSG-Ni_{5mmol}, including its Selected Area Diffraction (SAED) pattern in different magnifications. Figure 3 (a) shows the TEM image, including the Selected Area Diffraction (SAED) pattern of the CSG-$Ni_{5\ mmol}$ sample (inset). In the image, it can be seen that three typical rings are associated with the crystalline planes of (002), (101), and (110). The dotted ring pattern of SAED of CSG-Ni_{5mmol} corresponds to a single crystal followed by a polycrystalline-like material. The nearly bold ring embedded by a white-dotted point pattern of SAED (inset) indicated the polycrystalline-like pattern. It is obvious that the sample is a polycrystalline-like material. The higher magnification of the CSG-Ni_{5mmol} TEM image is shown in Figure 3(b). It clearly shows the number of highly oriented stacked carbon layers, which confirms the formation of the graphitic carbon structure. The plot profile (Figure 3c, inset) of the selected line is executed to measure the interplanar spacing of the carbon layer. Ten peaks of the plot profile correspond to ten layers of stacked carbon plane in the range of 3.4 nm. Based on the analysis of the selected line profile of the HR-TEM image, the interplanar spacing of the carbon layer is ~0.34 nm, which is in agreement with $d_{(002)}$ calculated from XRD data (~0.337 nm).

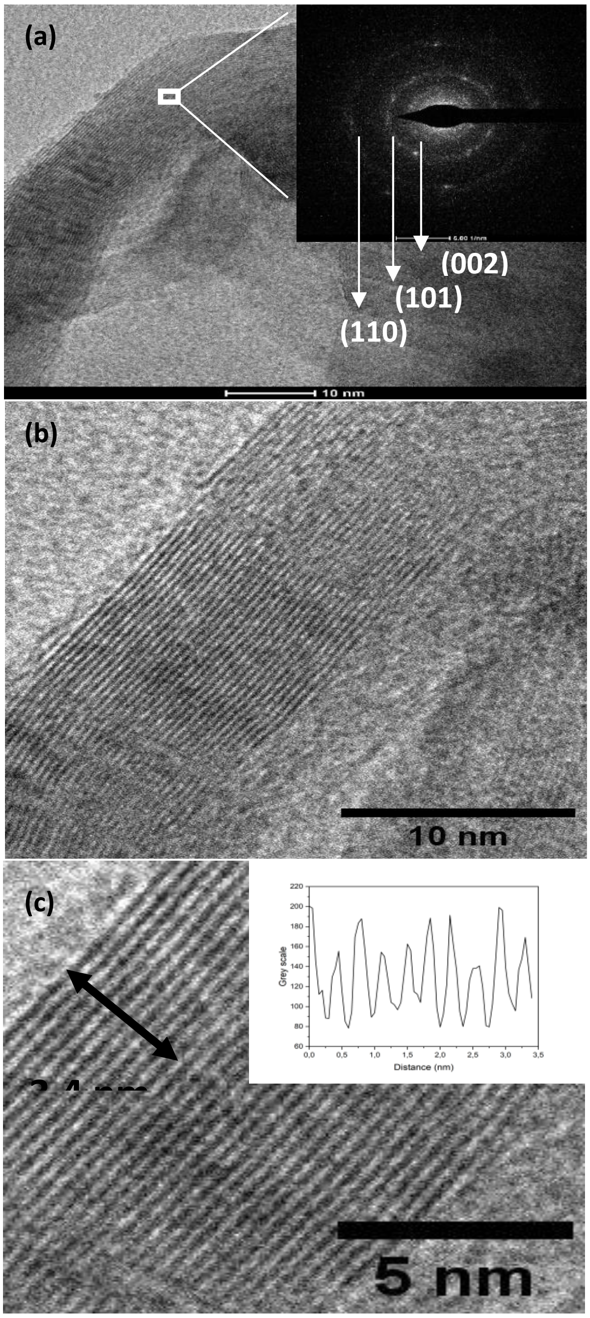

Figure 1. TEM Images of CSG-Ni5mmol and Its SAED Pattern (inset) (a), HR-TEM Images of CSG-Ni5mmol at Different Magnifications (b-c). Plot Profile at Selected Line (c,Inset).

The entire process in this research focuses on initial studies of the success of nickel catalyzation to convert biomass to highly ordered biomass graphitic carbon with low-temperature operation. Several types of metals as catalysts are highly recommended for research on various types of carbon biomass. In addition, studies about the utilization of graphite biomass in various strategic fields, such as energy (lithium-ion battery anode) and the environment (water treatment), are highly recommended.

CONCLUSION

High-ordered biomass graphite from coconut shells has been successfully synthesized using the metal catalytic-graphitization method with nickel as a catalyst. The metal catalyzation method was confirmed to have a lower graphitization temperature than ancient graphitization methods. This work reported that nickel impregnation has successfully facilitated graphitization at such a low temperature, ~ 1200 °C. The X-RD analysis confirmed that CSG and CSG-Ni_{2mmol} are amorphous materials. CSG-Ni_{3mmol} and CSG-Ni_{5mmol} are graphitic materials with DOG of 70.42 and 71.96, respectively. That clarified that a sufficient amount of nickel is essential to attain graphitization. Raman spectroscopy analysis also confirmed that nickel impregnation promoted graphitization, which enhanced the sp^2 carbon bond indicated by increasing the I_G/I_D value. The atomic morphology of CSG-Ni showed by TEM images confirmed the polycrystalline-like pattern of SAED. Furthermore, the high-ordered graphitic carbon layers were also observed by TEM images. The interplanar spacing of (002) was also calculated using plot profile analysis of the HR-TEM image. The interplanar spacing value is ~ 0.34 nm, which agrees with the XRD result.

ACKNOWLEDGMENT

This work is supported by funding from BOPTN UIN Syarif Hidayatullah Jakarta, Ministry of Religious Affairs of Indonesia. The author would also like to thank the Physics Laboratory Center of the National Research and Innovation Agency, Indonesia, and Green Laboratory, Bandung, Indonesia.

AUTHOR CONTRIBUTIONS

Biaunik Niski Kumila: Conceptualization, Methodology, Formal Analysis, Resources, Writing-Original Draft, Validation and Supervision; Farhan Aditya: Methodology, Formal Analysis, Resources and Investigation, Writing-Review Editing; Fredina Destyorini: Conceptualization, Methodology, Formal Analysis and Supervision; Fitri Nur Indah Sari, Dhita Azzahra, Hamdan Hadi Kusuma: Data Curation, Project Administration and Supervision

DECLARATION OF COMPETING INTEREST

The authors declare that they have no known competing financial interests or personal relationships that could have appeared to influence the work reported in this paper.

REFERENCES

[1] Thapaliya BP, Luo H, Halstenberg P, Meyer HM, Dunlap JR, and Dai S. Low-Cost Transformation of Biomass-Derived Carbon to high-Performing Nano-Graphite Via Low-Temperature Electrochemical Graphitization. *ACS Applied Materials and Interfaces*. 2021; **13**(3): 4393–4401. DOI: https://doi.org/10.1021/acsami.0c19395.

[2] Chen Y, Guo X, Liu A, Zhu H, Ma T. Recent Progress in Biomass-Derived Carbon Materials Used for Secondary Batteries. *Sustainable Energy and Fuels*. 2021; **5**(12): 3017–3038. DOI: https://doi.org/10.1039/D1SE00265A.

[3] Cai W, Zhu Y, Li X, Piner RD, and Ruoff RS. Large Area Few-Layer Graphene/Graphite Films as Transparent Thin Conducting Electrodes. *Applied Physics Letter*. 2009; **95**(12): 123115. DOI: https://doi.org/10.1063/1.3220807.

[4] Xu J, Wang X, Yuan N, Hu B, Ding J, and Ge S. Graphite-Based Lithium Ion Battery with Ultrafast Charging and Discharging and Excellent Low Temperature Performance. *Journal of Power Sources*. 2019; **430**: 74–79. DOI: https://doi.org/10.1016/j.jpowsour.2019.05.024.

[5] Hu G, Yu R, Liu Z, Yu Q, Zhang Y, Chen Q, et al. Surface Oxidation Layer-Mediated Conformal Carbon Coating on Si Nanoparticles for Enhanced Lithium Storage. *ACS Applied Materials and Interfaces*. 2021; **13**(3): 3991–3998. DOI: https://doi.org/10.1021/acsami.0c19673.

[6] Kim D, Ahmed T, Crossley K, Baldwin JK, Shin SHR, Kim Y, et al. A Controlled Nucleation and Growth of Si Nanowires by Using A Tin Diffusion Barrier Layer for Lithium-Ion Batteries. *Nanoscale Advances*. 2022; **4**(8): 1962–1969. DOI: https://doi.org/10.1039/D1NA00844G.

[7] Asenbauer J, Eisenmann T, Kuenzel M, Kazzazi A, Chen Z, and Bresser D. The Success Story of Graphite as A Lithium-Ion Anode Material-Fundamentals, Remaining Challenges, and Recent Developments Including Silicon (Oxide) Composites. *Sustainable Energy and Fuels*. 2020; **4**(11): 5387–5416. DOI: https://doi.org/10.1039/D0SE00175A.

[8] Sun Z and Chang H. Graphene and Graphene-like Two-Dimensional Materials in Photodetection: Mechanisms and Methodology. *ACS Nano*. 2014; **8**(5):4133–4156. DOI: https://doi.org/10.1021/nn500508c.

[9] Nazir A, Le HTT, Kasbe A, and Park CJ. Si Nanoparticles Confined Within a Conductive 2D Porous Cu-Based Metal–Organic Framework ($Cu_3(HITP)_2$) As Potential Anodes for High-Capacity Li-Ion Batteries. *Chemical Engineering Journal*. 2021; **405**(6): 126963. DOI: https://doi.org/10.1016/j.cej.2020.126963.

[10] Yang Y, Wu S, Zhang Y, Liu C, Wei X, Luo D, and Lin Z. Towards Efficient Binders for Silicon Based Lithium-Ion Battery Anodes. *Chemical Engineering Journal*. 2021; **406**: 126807. DOI: https://doi.org/10.1016/j.cej.2020.126807.

[11] Yim CH, Courtel FM, Abu-Lebdeh Y. A High Capacity Silicon-Graphite Composite as Anode for Lithium-Ion Batteries Using Low Content Amorphous Silicon and Compatible Binders. *Journal of Materials Chemistry A*. 2013; **1**(28): 8234–8243. DOI: https://doi.org/10.1039/C3TA10883J.

[12] Franklin RE. Crystallite Growth in Graphitizing and non-Graphitizing Carbons. *Proceedings of Royal Society A*. 1951; **209**(1097): 196–218. DOI: https://doi.org/10.1098/rspa.1951.0197.

[13] Feng P, Li J, Wang H, and Xu Z. Biomass-Based Activated Carbon and Activators: Preparation of Activated Carbon from Corncob by Chemical Activation with Biomass Pyrolysis Liquids. *ACS Omega*. 2020; **5**(37): 24064–24072. DOI: https://doi.org/10.1021/acsomega.0c03494.

[14] Gai L, Li J, Wang Q, Tian R, and Li K. Evolution of Biomass to Porous Graphite Carbon by Catalytic Graphitization. *Journal of Environmental Chemical Engineering*. 2021; **9**(6): 106678. DOI: https://doi.org/10.1016/j.jece.2021.106678.

[15] Banek NA, McKenzie KR, Abele DT, and Wagner MJ. Sustainable Conversion of Biomass to Rationally Designed Lithium-Ion Battery Graphite. *Scientific Reports*. 2022; **12**(1): 8080. DOI: https://doi.org/10.1038/s41598-022-11853-x.

[16] Suzuki K, Saito Y, Okazaki N, and Suzuki T. Graphite-Shell-Chains Selectively and Efficiently Produced from Biomass Rich in Cellulose and Chitin. *Scientific Reports*. 2020; **10**(1): 12131. DOI: https://doi.org/10.1038/s41598-020-69156-y.

[17] He W, Luo H, Jing P, Wang H, Xu C, Wu H, et al. Embedding Silicon in Biomass-Derived Porous Carbon Framework as High-Performance Anode of Lithium-Ion Batteries. *Journal of Alloys and Compounds*. 2022; **918**: 165364. DOI: https://doi.org/10.1016/j.jallcom.2022.165364.

[18] Destyorini F, Amalia WC, Irmawati Y, Hardiansyah A, Priyono S, Aulia F, et al. High Graphitic Carbon Derived from Coconut Coir Waste by Promoting Potassium Hydroxide in the Catalytic Graphitization Process for Lithium-Ion Battery Anodes. *Energy and Fuels*. 2022; **36**(10): 5444-5455. DOI: https://doi.org/10.1021/acs.energyfuels.2c00632.

[19] Osman NB, Shamsuddin N, and Uemura Y. Activated Carbon of Oil Palm Empty Fruit Bunch (EFB); Core and Shaggy. *Procedia Engineering*. 2016; **148**: 758–764. DOI: https://doi.org/10.1016/j.proeng.2016.06.610.

[20] Hidayu AR, Mohamad NF, Matali S, and Sharifah ASAK. Characterization of Activated Carbon Prepared from Oil Palm Empty Fruit Bunch Using BET and FT-IR Techniques. *Procedia Engineering*. 2013; **68**: 379–384. DOI: https://doi.org/10.1016/j.proeng.2013.12.195.

[21] Kamal AS, Othman R, and Jabarullah NH. Preparation and Synthesis of Synthetic Graphite from Biomass Waste: A Review. *Systematic Reviews in Pharmacy*. 2020; **11**(2): 881–894. Available from: https://www.sysrevpharm.org/abstract/preparation-and-synthesis-of-synthetic-graphite-from-biomass-waste-a-review-65651.html#cite.

[22] Wang R, Lu G, Qiao W, and Yu J. Catalytic Graphitization of Coal-Based Carbon Materials with Light Rare Earth Elements. *Langmuir*. 2016; **32**(34): 8583–8592. DOI: https://doi.org/10.1021/acs.langmuir.6b02000.

[23] Maiaugree W, Lowpa S, Towannang M, Rutphonsan P, Tangtrakarn A, et al. A dye sensitized solar cell using natural counter electrode and natural dye derived from mangosteen peel waste. *Science Reports*. 2015; 5: 15230. DOI: https://doi.org/10.1038/srep15230.

[24] Keppetipola NM, Dissanayake M, Dissanayake P, Karunarathne B, Dourges MA, Talaga D, et al. Graphite-Type Activated Carbon from Coconut Shell: A Natural Source for Eco-Friendly Non-Volatile Storage Devices. *RSC Advances*. 2021; **11**(5): 2854–2865. DOI: https://doi.org/10.1039/D0RA09182K.

[25] Mas'udah KW, Nugraha IMA, Abidin S, Mufid A, Astuti F, and Darminto. Solution of Reduced Graphene Oxide Synthesized from Coconut Shells and Its Optical Properties. *AIP Conference Proceedings*. 2016; **1725**: 020045. DOI: https://doi.org/10.1063/1.4945499.

[26] Sundarababu J, Anandan SS, and Griskevicius P. Evaluation of Mechanical Properties of Biodegradable Coconut Shell/Rice Husk Powder Polymer Composites for Light Weight Applications. *Materials Today: Proceedings*. 2021; **39**(4): 1241–1247. DOI: https://doi.org/10.1016/j.matpr.2020.04.095.

[27] Udhayasankar R and Karthikeyan B. A Review on Coconut Shell Reinforced Composites. *International Journal Chemtech Research*. 2015; **8**(11): 624–637. Available from: https://sphinxsai.com/2015/ch_vol8_no11/3/(624-637)V8N11CT.pdf.

[28] Khuluk RH, Rahmat A, Buhani, and Suharso. Removal of Methylene Blue by Adsorption onto Activated Carbon from Coconut Shell (Cocous Nucifera L.). *Indonesian Journal of Science and Technology*. 2019; **4**(2): 229–240. DOI: https://doi.org/10.17509/ijost.v4i2.18179.

[29] Wang J and Kaskel S. KOH Activation of Carbon-Based Materials for Energy Storage. *Journal of Materials Chemistry*. 2012; **22**: 23710–23725. DOI: https://doi.org/10.1039/C2JM34066F.

[30] Hunter RD, Ramírez-Rico J, and Schnepp Z. Iron-Catalyzed Graphitization for The Synthesis of Nanostructured Graphitic Carbons. *Journal of Materials Chemistry A*. 2022; **10**(9): 4489–4516. DOI: https://doi.org/10.1039/D1TA09654K.

[31] Hoekstra J, Beale AM, Soulimani F, Versluijs-Helder M, Geus JW, and Jenneskens LW. Base Metal Catalyzed Graphitization of Cellulose: A Combined Raman Spectroscopy, Temperature-Dependent X-Ray Diffraction and High-Resolution Transmission Electron Microscopy Study. *Journal of Physical Chemistry C*. 2015; **119**(19):10653–10661. DOI: https://doi.org/10.1021/acs.jpcc.5b00477.

[32] Liu Y, Liu Q, Gu J, Kang D, Zhou F, Zhang W, Wu Y, and Zhang D. Highly Porous Graphitic Materials Prepared by Catalytic Graphitization. *Carbon* 2013; **64**: 132–140. DOI: https://doi.org/10.1016/j.carbon.2013.07.044.

[33] Sun H, Sun K, Wang F, Liu Y, Ding L, Xu W, Sun S, and Jiang J. Catalytic Self-Activation of Ca-Doped Coconut Shell for In-Situ Synthesis of Hierarchical Porous Carbon Supported CaO Transesterification Catalyst. *Fuel*. 2021; **285**: 119192. DOI: https://doi.org/10.1016/j.fuel.2020.119192.

[34] Destyorini F, Irmawati Y, Hardiansyah A, Widodo H, Yahya IND, Indayaningsih N, Yudianti R, Hsu Y-I, and Uyama H. Formation of Nanostructured Graphitic Carbon from Coconut Waste Via Low-Temperature Catalytic Graphitisation. *Engineering Science and Technology, an International Journal*. 2021; **24**(2): 514–523. DOI: https://doi.org/10.1016/j.jestch.2020.06.011.

[35] Fuertes AB and Alvarez S. Graphitic Mesoporous Carbons Synthesised Through Mesostructured Silica Templates. *Carbon*. 2004; **42**(15): 3049–3055. DOI: https://doi.org/10.1016/j.carbon.2004.06.020.

[36] Wachid FM, Perkasa AY, Prasetya FA, Rosyidah N, and Darminto. Synthesis and Characterization of Nanocrystalline Graphite from Coconut Shell with Heating Process. *AIP Conference Proceedings*. 2014; **1586**: 202–206. DOI: https://doi.org/10.1063/1.4866759.

[37] Mukimin A, Yuliasni R, Zen N, Wicaksono KA, Fatkhurahman JA, Vistanty H, and Malik RA. Synthesis of Graphite Porous Electrode Based on Coconut Shell as A Potential Cathode in Bioelectrosyntesis Cell. *Indonesian Journal of Chemistry*. 2019; **19**(2): 413–421. DOI: https://doi.org/10.22146/ijc.37550.

[38] Kumila BN, Zaidah N, and Kusuma HH. Green Reduction of Graphene Oxide (GO) from Coconut Shell Using Rose Water in Various Temperature. *Jurnal Fisika dan Aplikasinya*. 2022; **18**(2): 48-52. DOI: http://dx.doi.org/10.12962/j24604682.v18i2.12277.

[39] Barnakov CN, Khokhlova GP, Popova AN, Sozinov SA, and Ismagilov ZR. XRD Characterization of The Structure of Graphites and Carbon Materials Obtained by The Low-Temperature Graphitization of Coal Tar Pitch. *Eurasian Chemico-Technological Journal*. 2015; **17**(2): 87–93. DOI: http://dx.doi.org/10.18321/ectj198.

[40] Zou L, Huang B, Huang Y, Huang Q, and Wang C. An Investigation of Heterogeneity of The Degree of Graphitization in Carbon-Carbon Composites. Mater Chem Phys. 2003; **82**(3): 654–662. DOI: https://doi.org/10.1016/S0254-0584(03)00332-8.

[41] Käärik M, Arulepp M, Karelson M, and Leis J. The Effect of Graphitization Catalyst on The Structure and Porosity of SiC Derived Carbons. *Carbon*. 2008; **46**(12): 1579–1587. DOI: https://doi.org/10.1016/j.carbon.2008.07.003.

[42] Umerah CO, Kodali D, Head S, Jeelani S, and Rangari VK. Synthesis of Carbon from Waste Coconutshell and Their Application as Filler in Bioplast Polymer Filaments for 3D Printing. Composites Part B: Engineering. 2020; **202**: 108428. DOI: https://doi.org/10.1016/j.compositesb.2020.108428.

[43] Kim J, Lee J, Choi Y, and Jo C. Synthesis of Hierarchical Linearly Assembled Graphitic Carbon Nanoparticles Via Catalytic Graphitization in SBA-15. *Carbon*. 2014; **75**: 95–103. DOI: https://doi.org/10.1016/j.carbon.2014.03.039.

[44] Li ZQ, Lu CJ, Xia ZP, Zhou Y, and Luo Z. X-Ray Diffraction Patterns of Graphite and Turbostratic Carbon. *Carbon*. 2007; **45**(8): 1686–1695. DOI: https://doi.org/10.1016/j.carbon.2007.03.038.

[45] Meng Y, Contescu CI, Liu P, Wang S, Lee SH, Guo J, et al. Understanding the Local Structure of Disordered Carbons from Cellulose and Lignin. *Wood Science and Technology*. 2021; **55**(3): 587–606. DOI: https://doi.org/10.1007/s00226-021-01286-6.

[46] Xu J, Liu J, Ling P, Zhang X, Xu K, He L, et al. Raman Spectroscopy of Biochar from the Pyrolysis of Three Typical Chinese Biomasses: A Novel Method for Rapidly Evaluating the Biochar Property. *Energy*. 2020; **202**: 117644. DOI: https://doi.org/10.1016/j.energy.2020.117644.

[47] Compton OC and Nguyen ST. Graphene Oxide, Highly Reduced Graphene Oxide, and Graphene: Versatile Building Blocks for Carbon-Based Materials. *Small*. 2010; **6**(6): 711–723. DOI: https://doi.org/10.1002/smll.200901934.

[48] Hassinen J, Kauppila J, Leiro J, Määttänen A, Ihalainen P, Peltonen J, and Lukkari J. Low-Cost Reduced Graphene Oxide-Based Conductometric Nitrogen Dioxide-Sensitive Sensor on Paper. *Analytical and Bioanalytical Chemistry*. 2013; **405**(11): 3611–3617. DOI: https://doi.org/10.1007/s00216-013-6805-5.

[49] Sarkar SK, Raul KK, Pradhan SS, Basu S, and Nayak A. Magnetic Properties of Graphite Oxide and Reduced Graphene Oxide. *Physica E: Low Dimensional Systems and Nanostructures*. 2014; **64**: 78–82. DOI: https://doi.org/10.1016/j.physe.2014.07.014.

[50] Oya A and Otani S. Catalytic Graphitization of Carbons by Various Metals. *Carbon*. 1979; **17**(2): 131–137. DOI: https://doi.org/10.1016/0008-6223(79)90020-4.